Polaron-transformed dissipative Lipkin-Meshkov-Glick model

Wassilij Kopylov[*] and Gernot Schaller [†]

Institut für Theoretische Physik, Technische Universität Berlin, D-10623 Berlin, Germany

We investigate the Lipkin-Meshkov-Glick model coupled to a thermal bath. Since the isolated model itself exhibits a quantum phase transition, we explore the critical signatures of the open system. Starting from a system-reservoir interaction written in positive-definite form, we find that the position of the critical point remains unchanged, in contrast to the popular mean-field prediction. Technically, we employ the polaron transform to be able to study the full crossover regime from the normal to the symmetry-broken phase, which allows us to investigate the fate of quantum-critical points subject to dissipative environments. The signatures of the phase transition are reflected in observables such as magnetization, stationary mode occupation, or waiting-time distributions.

I. INTRODUCTION

In closed systems, quantum phase transitions (QPTs) are defined as nonanalytic changes of the ground-state energy when a control parameter other than temperature is varied across a critical point [1]. They are accompanied by nonanalytic changes in observables or correlation functions [2–4] and form a fascinating research area on their own.

Nowadays, it is possible to study such QPTs in experimental setups with cold atoms [5–9], which provide a high degree of control and allow one to test theoretical predictions. However, each experimental setup is an open system, such that the impact of the reservoir on the QPT should not be neglected. To the contrary, the presence of a reservoir can fundamentally change the nature of the QPT. For example, in the famous Dicke phase transition, it is the presence of the reservoir that actually creates a QPT via the environmental coupling of a collective spin [10].

With the renewed interest in quantum thermodynamics, it has become a relevant question whether QPTs can be put to use, e.g., as working fluids of quantum heat engines [11–14]. This opens another broad research area of dissipative QPTs in nonequilibrium setups. Here, the nonequilibrium configuration can be implemented in different ways, e.g., by periodic driving [15–17], quenching [18–20], coupling to reservoirs [21–23], or a combination of these approaches [24,25]. One has even considered feedback control of such quantum-critical systems [26–30].

All of these extensions should, however, be applied in combination with a reliable microscopic description of the system-reservoir interaction. For example, in the usual derivation of Lindblad master equations, one assumes that the system-reservoir interaction is weak compared to the splitting of the system energy levels [21,31]. In particular in the vicinity of a QPT—where the energy gap above the ground state

vanishes—this condition cannot be maintained. Therefore, while in particular the application of the secular approximation leads to a Lindblad-type master equation preserving the density matrix properties, it has the disadvantage that its range of validity is typically limited to noncritical points or to finite-size scaling investigations [32,33]. In principle, the weak-coupling restriction can be overcome with different methods, such as reaction-coordinate mappings [34–36]. These, however, come at the price of increasing the dimension of the system, which renders analytic treatments of already complex systems difficult.

In this paper, we are going to study, using the example of the Lipkin-Meshkov-Glick (LMG) model, how a QPT is turned dissipative by coupling the LMG system [37] to a large environment. To avoid the aforementioned problems, we use a polaron [38–42] method, which allows us to address the strong-coupling regime [34,43–49] without increasing the number of degrees of freedom that need explicit treatment. In particular, we show that for our model, the position of the QPT is robust in the presence of dissipation. We emphasize that the absence of a reservoir-induced shift— in contrast to mean-field predictions [23,50–55]—is connected with starting from a Hamiltonian with a lower spectral bound and holds without additional approximation. Our work is structured as follows. In Sec. II, we introduce the dissipative LMG model, and in Sec. III, we show how to diagonalize it globally using the Holstein-Primakoff transformation. There, we also derive a master equation in both the original and polaron frames, and show that the QPT cannot be modeled within the first and that the QPT position is not shifted within the latter approach. Finally, we discuss the effects near the QPT by investigating the excitations in the LMG system and the waiting-time distribution of emitted bosons in Sec. IV.

II. MODEL

A. Starting Hamiltonian

The isolated LMG model describes the collective interaction of N two-level systems with an external field and among

---

[*]kopylov@itp.tu-berlin.de

[†]gernot.schaller@tu-berlin.de

themselves. In terms of the collective spin operators

$$J_\nu = \frac{1}{2} \sum_{m=1}^{N} \sigma_\nu^{(m)}, \quad \nu \in \{x, y, z\}, \tag{1}$$

and $J_\pm = J_x \pm i J_y$, with $\sigma_\nu^{(m)}$ denoting the Pauli matrix of the mth spin, the anisotropic LMG Hamiltonian reads [56]

$$H_{\text{LMG}}(h, \gamma_x) = -h J_z - \frac{\gamma_x}{N} J_x^2, \tag{2}$$

where h is the strength of a magnetic field in the z direction and γ_x is the coupling strength between each pair of two-level systems. As such, it can be considered a quantum generalization of the Curie-Weiss model [57]. Throughout this paper, we consider only the subspace with the maximum angular momentum $j = \frac{N}{2}$, where the eigenvalues of the angular momentum operator $J^2 = J_x^2 + J_y^2 + J_z^2$ are given by $j(j + 1)$. Studies of the LMG model are interesting not only due to its origin in the nuclear context [37,58,59], but also due to its experimental realization with cold atoms and high possibility of control [8]. In particular, the existence of a QPT at $\gamma_x^{\text{cr}} = h$ with a nonanalytic ground-state energy density has raised the interest of the community [60–63]: For $\gamma_x < \gamma_x^{\text{cr}}$, the system has a unique ground state, which we denote as the *normal phase* further on. In contrast, for $\gamma_x > \gamma_x^{\text{cr}}$, it exhibits a *symmetry-broken phase* [2,64], where, e.g., the eigenvalues become pairwise degenerate and the J_z expectation exhibits a bifurcation [19,65]. Strictly speaking, the QPT is found only in the thermodynamic limit (for $N \to \infty$), for finite-size N smoothing effects in the QPT signatures will appear [66–68].

Here, we want to investigate the LMG model embedded in an environment of bosonic oscillators c_k with frequencies ν_k. The simplest nontrivial embedding preserves the conservation of the total angular momentum and allows for energy exchange between system and reservoir. Here, we constrain ourselves for simplicity to the case of a J^x coupling. Furthermore, to ensure that the Hamiltonian has a lower spectral bound for all values of the system-reservoir coupling strength, we write the interaction in terms of a positive operator,

$$H_{\text{tot}} = H_{\text{LMG}}(h, \gamma_x) + \sum_k \nu_k \left(c_k^\dagger + \frac{g_k}{\sqrt{N} \nu_k} J_x \right)$$
$$\times \left(c_k + \frac{g_k}{\sqrt{N} \nu_k} J_x \right). \tag{3}$$

Here, $g_k > 0$ represent emission and absorption amplitudes (a possible phase can be absorbed in the bosonic operators), and the factor $N^{-1/2}$ needs to be included to obtain a meaningful thermodynamic limit $N \to \infty$, but can also be motivated from the scaling of the quantization volume $V \propto N$. Since the LMG Hamiltonian has a lower bound, the spectrum of this Hamiltonian H_{tot} is (for finite N) then bounded from below for all values of the coupling strength g_k. Upon expansion and sorting of spin and bosonic operators, this form implicates an effective rescaling of the system Hamiltonian $H_{\text{LMG}}(h, \tilde{\gamma}_x)$ with a renormalized spin-spin interaction,

$$\tilde{\gamma}_x = \gamma_x - \sum_k \frac{g_k^2}{\nu_k}, \tag{4}$$

which indeed leads to a shift of the critical point within a naive treatment.

B. Local LMG diagonalization

In the thermodynamic limit, Eq. (2) can be diagonalized using the Holstein-Primakoff transform, which maps collective spins to bosonic operators b [23,69,70],

$$J_+ = \sqrt{N - b^\dagger b}\, b, \quad J_- = b^\dagger \sqrt{N - b^\dagger b},$$
$$J_z = \frac{N}{2} - b^\dagger b. \tag{5}$$

However, to capture both phases of the LMG Hamiltonian, one has to account for the macroscopically populated ground state in the symmetry-broken phase. This can be included with the displacement $b = \sqrt{N} \alpha + a$, with complex α in Eq. (5), where $N|\alpha|^2$ is the classical mean-field population of the mode [23,62,70] and a is another bosonic annihilation operator. The next step is then to expand for either phase given by Eq. (2) with the inserted transformation (5) in terms of $1/\sqrt{N}$ for $N \gg 1$ (see Appendix A), which yields a decomposition of the Hamiltonian

$$H_{\text{LMG}}^{\text{HP}}(h, \gamma_x) = N H_0^{\text{HP}} + \sqrt{N} H_1^{\text{HP}} + H_2^{\text{HP}} + O\left(\frac{1}{\sqrt{N}}\right), \tag{6}$$

with individual terms depending on the phase:

$$H_0^{\text{HP}} = \begin{cases} -\frac{h}{2} & : \gamma_x < \gamma_x^{\text{cr}} \\ -\frac{h^2 + \gamma_x^2}{4\gamma_x} & : \gamma_x > \gamma_x^{\text{cr}}, \end{cases}$$

$$H_1^{\text{HP}} \overset{!}{=} \begin{cases} 0 & : \gamma_x < \gamma_x^{\text{cr}} \\ 0 & : \gamma_x > \gamma_x^{\text{cr}}, \end{cases}$$

$$H_2^{\text{HP}} = \begin{cases} (h - \frac{\gamma_x}{2}) a^\dagger a - \frac{\gamma_x}{4}(a^2 + a^{\dagger 2}) - \frac{\gamma_x}{4} & : \gamma_x < \gamma_x^{\text{cr}} \\ +\frac{5\gamma_x - 3h}{4} a^\dagger a + \frac{3\gamma_x - 5h}{8}(a^2 + a^{\dagger 2}) & : \gamma_x > \gamma_x^{\text{cr}} \\ +\frac{\gamma_x - 3h}{8}. \end{cases}$$
$$\tag{7}$$

We demand, in both phases, that H_1^{HP} is always zero. Technically, this enforces that only terms quadratic in the creation and annihilation operators occur in the Hamiltonian. Physically, this enforces that we expand around the correct ground state, i.e., in the final basis, the ground state is the state with a vanishing quasiparticle number. This requirement is trivially fulfilled in the normal phase with $\alpha = 0$, but requires a finite real value of the mean field α in the symmetry-broken phase [23,62,70], altogether leading to a phase-dependent displacement,

$$\alpha(h, \gamma_x) = \sqrt{\frac{1}{2}\left(1 - \frac{h}{\gamma_x}\right)} \Theta(\gamma_x - h), \tag{8}$$

which approximates $H_{\text{LMG}}^{\text{HP}}$ by a harmonic oscillator near its ground state. Here we note that $-\alpha(h, \gamma_x)$ is also a solution. The mean-field expectation value already allows one to see the signature of the phase transition in the closed LMG model at $\gamma_x = h$, since α is only finite for $\gamma_x > h$ and is zero elsewhere.

Since, up to corrections that vanish in the thermodynamic limit, the Hamiltonian defined by Eq. (6) is quadratic in a, it can in either phase be diagonalized by a rotation of

TABLE I. Parameters of the diagonalization procedure of the LMG model $H_{\text{LMG}}(h, \gamma_x)$ for the normal phase ($\gamma_x < h$, second column) and for the symmetry-broken phase ($\gamma_x > h$, last column). In both phases, the d operators correspond to fluctuations around the mean-field value α, which is zero only in the normal phase.

	Normal: $\gamma_x < h$	Symmetry broken: $\gamma_x > h$
b	$\sqrt{N}\alpha(h, \gamma_x) + \cosh[\varphi(h, \gamma_x)]d + \sinh[\varphi(h, \gamma_x)]d^\dagger$	
$\varphi(h, \gamma_x)$	$\frac{1}{4}\ln\left(\frac{h}{h-\gamma_x}\right)$	$\frac{1}{4}\ln\left[\frac{\gamma_x+h}{4(\gamma_x-h)}\right]$
$\alpha(h, \gamma_x)$	0	$\sqrt{\frac{1}{2}\left(1 - \frac{h}{\gamma_x}\right)}$
$\omega(h, \gamma_x)$	$\sqrt{h(h-\gamma_x)}$	$\sqrt{\gamma_x^2 - h^2}$
$C_1(h, \gamma_x)$	$\frac{h}{2}$	$\frac{h^2+\gamma_x^2}{4\gamma_x}$
$C_2(h, \gamma_x)$	$\frac{1}{2}\left[\sqrt{h(h-\gamma_x)} - h\right]$	$\frac{1}{2}\left(\sqrt{\gamma_x^2 - h^2} - \gamma_x\right)$

the old operators $a = \cosh(\varphi)d + \sinh(\varphi)d^\dagger$ with $\varphi \in \mathbb{R}$ to new bosonic operators d. The system Hamiltonian $H_{\text{LMG}}^{\text{HP}}$ then transforms into a single harmonic oscillator, where the frequency ω and ground-state energy are functions of h and γ_x,

$$H_{\text{LMG}}^{\text{HP}}(h, \gamma_x) = \omega(h, \gamma_x)d^\dagger d + C_2(h, \gamma_x) - NC_1(h, \gamma_x)$$
$$+ O\left(\frac{1}{\sqrt{N}}\right). \tag{9}$$

The actual values of the excitation energies $\omega(h, \gamma_x)$ and the constants $C_i(h, \gamma_x)$ are summarized in Table I. Figure 1 confirms that the thus obtained spectra from the bosonic representation agree well with finite-size numerical diagonalization when N is large enough.

First, one observes for consistency that the trivial spectra deeply in the normal phase ($\gamma_x \approx 0$) or deeply in the symmetry-broken phase ($h \approx 0$) are reproduced. In addition,
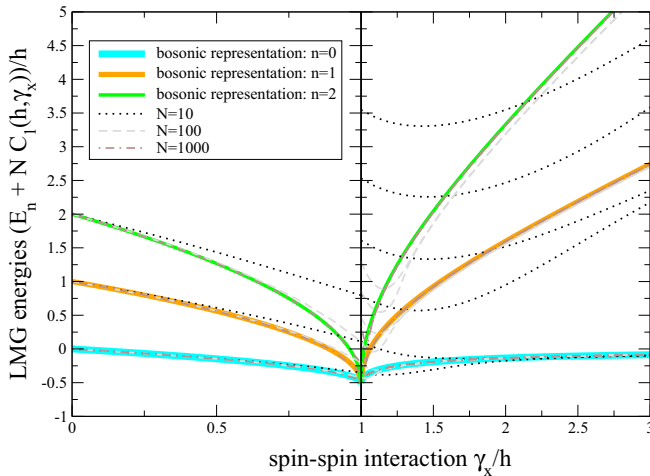

FIG. 1. Lower part of the isolated LMG model spectrum for finite-size numerical diagonalization of Eq. (2) (thin curves) and using the bosonic representation (bold curves) based on Eq. (9) for the three lowest energies. For large N, the spectra are nearly indistinguishable. In the symmetry-broken phase (right), two numerical eigenvalues approach the same oscillator solution. These correspond to the two different parity sectors, formally represented by two possible displacement solutions $\pm\alpha(h, \gamma_x)$ in Eq. (8).

we see that at the QPT $\gamma_x = \gamma_x^{\text{cr}} = h$, the excitation frequency ω vanishes as expected, which is also reflected, e.g., in the dashed curve in Fig. 3(a). For consistency, we also mention that all oscillator energies E_n are continuous at the critical point $\gamma = h$. Furthermore, the second derivative with respect to γ_x of the continuum ground-state energy per spin, $\lim_{N\to\infty} E_0/N$, is discontinuous at the critical point, classifying the phase transition as second order. Finally, we note that this treatment does not capture the excited-state quantum phase transitions present in the LMG model as we are only concerned with the lower part of the spectrum.

III. MASTER EQUATION

We first perform the derivation of the conventional Born-Markov-secular (BMS) master equation in the usual way, starting directly with Eq. (3) [22,23,71]. Afterwards, we show that a polaron transform also allows one to treat regions near the critical point.

A. Conventional BMS master equation

The conventional BMS master equation is derived in the energy eigenbasis of the system, i.e., the LMG model with renormalized spin-spin interaction $\tilde{\gamma}_x$, in order to facilitate the secular approximation. In this eigenbasis, the master equation has a particularly simple form.

Applying the very same transformations (that diagonalize the closed LMG model) to its open version (3), we arrive at the generic form

$$H_{\text{tot}}^{\text{HP}} = H_{\text{LMG}}^{\text{HP}}(h, \tilde{\gamma}_x) + \sum_k v_k c_k^\dagger c_k + [A(h, \tilde{\gamma}_x)(d + d^\dagger)$$
$$+ \sqrt{N}Q(h, \tilde{\gamma}_x)]\sum_k g_k(c_k + c_k^\dagger), \tag{10}$$

where we note that the LMG Hamiltonian is now evaluated at the shifted interaction (4). The phase-dependent numbers A and Q are defined in Table II. In particular, in the normal phase we have $Q = 0$, and we recover the standard problem of a harmonic oscillator weakly coupled to a thermal reservoir. In the symmetry-broken phase, we have $Q \neq 0$, such that the shift term in the interaction Hamiltonian formally diverges as $N \to \infty$, and a naive perturbative treatment does not apply. Some thought, however, shows that this term can be transformed away by applying yet another displacement for both system and reservoir modes $d \to d + \sigma$ and $c_k \to c_k + \sigma_k$

TABLE II. Additional parameters of the diagonalization procedure for the derivation of the master equation in the original frame for the normal phase ($\tilde{\gamma}_x < h$, second column) and for the symmetry-broken phase ($\tilde{\gamma}_x > h$, last column). Note that as compared to the closed model in Table I, functions are evaluated at the shifted interaction (4).

	Normal: $\tilde{\gamma}_x < h$	Symmetry broken: $\tilde{\gamma}_x > h$
$C_3(h, \tilde{\gamma}_x)$	1	$\frac{\sqrt{2}h}{\sqrt{\tilde{\gamma}_x(\tilde{\gamma}_x+h)}}$
$A(h, \tilde{\gamma}_x)$	$\frac{C_3(h, \tilde{\gamma}_x)}{2}\exp[\varphi(h, \tilde{\gamma}_x)]$	
$Q(h, \tilde{\gamma}_x)$	$\alpha(h, \tilde{\gamma}_x)\sqrt{1 - \alpha^2(h, \tilde{\gamma}_x)}$	

with $\sigma, \sigma_k \in \mathbb{C}$ chosen such that all terms linear in creation and annihilation operators vanish in the total Hamiltonian. This procedure does not change the energies of either system or bath operators, such that eventually the master equation in the symmetry-broken phase is formally equivalent to the one in the normal phase, and the interaction proportional to Q is not problematic.

Still, when one approaches the critical point from either side, the system spacing ω closes in the thermodynamic limit, which makes the interaction Hamiltonian at some point equivalent or even stronger than the system Hamiltonian. Even worse, one can see that simultaneously, the factor $A \sim e^{+\varphi}$ in the interaction Hamiltonian diverges at the critical point, such that a perturbative treatment is not applicable there. Therefore, one should consider the results of the naive master equation in the thermodynamic limit $N \to \infty$ with caution. The absence of a microscopically derived master equation near the critical point is a major obstacle in understanding the fate of quantum criticality in open systems.

Ignoring these problems, one obtains a master equation having the standard form for a harmonic oscillator coupled to a thermal reservoir,

$$\dot{\rho}(t) = -i[H^{\mathrm{HP}}_{\mathrm{LMG}}(h, \tilde{\gamma}_x), \rho] + F_e \mathcal{D}(d)\rho + F_a \mathcal{D}(d^\dagger)\rho,$$
$$F_e = A^2(h, \tilde{\gamma}_x)\Gamma(\omega(h, \tilde{\gamma}_x))[1 + n_B(\omega(h, \tilde{\gamma}_x))],$$
$$F_a = A^2(h, \tilde{\gamma}_x)\Gamma(\omega(h, \tilde{\gamma}_x))n_B(\omega(h, \tilde{\gamma}_x)). \quad (11)$$

Here, we have used the superoperator notation $\mathcal{D}(O)\rho \hat{=} O\rho O^\dagger - \frac{1}{2}\rho O^\dagger O - \frac{1}{2}O^\dagger O\rho$ for any operator O and

$$\Gamma(\omega) = 2\pi \sum_k g_k^2 \delta(\omega - \nu_k) \quad (12)$$

is the original spectral density of the reservoir, and $n_B(\omega) = [e^{\beta\omega} - 1]^{-1}$ is the Bose distribution with inverse reservoir temperature β. These functions are evaluated at the system transition frequency $\omega(h, \tilde{\gamma}_x)$. The master equation has the spontaneous and stimulated emission terms in F_e and the absorption term in F_a, and, due to the balanced Bose-Einstein function, these will, at the steady state, just thermalize the system at the reservoir temperature, as is generically found for such BMS master equations. Note that $H^{\mathrm{HP}}_{\mathrm{LMG}}$ from Eq. (11) is evaluated at the rescaled coupling $\tilde{\gamma}_x$. Therefore, the position of the QPT is at $\tilde{\gamma}_x^{\mathrm{cr}} = h$ and shifted to higher γ_x couplings; see Eq. (4). Similar shifts of the QPT position in dissipative quantum optical models are known, e.g., from mean-field treatments [50,72]. However, here we emphasize that we observe them as a direct consequence of ignoring the divergence of interaction around the phase transition in combination with the positive-definite form of the initial total Hamiltonian given by Eq. (3).

B. Polaron master equation

In this section, we apply a unitary polaron transform to the complete model, which has for other (noncritical) models been used to investigate the full regime of system-reservoir coupling strengths [73,74]. We will see that for a critical model, it can—while still bounded in the total coupling strength—be used to explore the system's behavior at the QPT position.

1. Polaron transform

We choose the following polaron transform U_p:

$$U_p = e^{-J_x\hat{B}}, \quad \hat{B} = \frac{1}{\sqrt{N}} \sum_k \frac{g_k}{\nu_k}(c_k^\dagger - c_k). \quad (13)$$

The total Hamiltonian (3) in the polaron frame then becomes

$$\bar{H}_{\mathrm{tot}} = U_p^\dagger H_{\mathrm{tot}} U_p$$
$$= -hDJ_z - \frac{\gamma_x}{N}J_x^2 + \sum_k \nu_k c_k^\dagger c_k$$
$$- h[J_z(\cosh(\hat{B}) - D) - iJ_y\sinh(\hat{B})]. \quad (14)$$

Here, γ_x is the original interaction of the local LMG model, and the renormalization of the external field D is defined via

$$D = \langle\cosh(\hat{B})\rangle = \mathrm{Tr}\left\{\cosh(\hat{B})\frac{e^{-\beta\sum_k \nu_k c_k^\dagger c_k}}{\mathrm{Tr}(e^{-\beta\sum_k \nu_k c_k^\dagger c_k})}\right\}$$
$$= \exp\left[-\frac{1}{N}\sum_k \left(\frac{g_k}{\nu_k}\right)^2\left(n_k + \frac{1}{2}\right)\right] > 0,$$
$$n_k = \frac{1}{e^{\beta\nu_k} - 1}. \quad (15)$$

It has been introduced to enforce that the expectation value of the system-bath coupling vanishes for the thermal reservoir state. More details on the derivation of Eq. (14) are presented in Appendix B.

The operator $\hat{B} \propto \frac{1}{\sqrt{N}}$ decays in the thermodynamic limit, such that for these studies, only the first few terms in the expansions of the $\sinh(\hat{B})$ and $\cosh(\hat{B})$ terms need to be considered.

Accordingly, the position of the QPT in the polaron frame is now found at the QPT of the closed model,

$$\gamma_x^{\mathrm{cr}} = hD \overset{N\to\infty}{\to} h. \quad (16)$$

Here, we have with $D \to 1$ implicitly assumed that the thermodynamic limit is performed in the system first. If a spectral density is chosen that vanishes faster than quadratically for small frequencies, the above replacement holds unconditionally (see below).

We emphasize again we observe the absence of a QPT shift as a result of a proper system-reservoir interaction with a lower spectral bound. Without such an initial Hamiltonian, the reservoir backaction would shift the dissipative QPT [50,72].

For the study of strong-coupling regimes, polaron transforms have also been applied, e.g., to single spin systems [73] and collective noncritical spin systems [74]. Treatments without a polaron transformation should be possible in our case too, by rewriting Eq. (3) in terms of reaction coordinates [35,36,75], leading to an open Dicke-type model.

In the thermodynamic limit, we can use that the spin operators J_ν scale, at worst, linearly in N to expand the interaction and D, yielding

$$\bar{H}_{\mathrm{tot}} \approx -h\left[1 - \frac{1}{N}\delta\right]J_z - \frac{\gamma_x}{N}J_x^2 + \sum_k \nu_k c_k^\dagger c_k$$
$$- h\left[\frac{J_z}{N}\left(\frac{1}{2}\bar{B}^2 + \delta\right) - i\frac{J_y}{\sqrt{N}}\bar{B}\right]$$

$$= -hJ_z - \frac{\gamma_x}{N}J_x^2 + \sum_k \nu_k c_k^\dagger c_k - h\left[\frac{J_z}{N}\frac{1}{2}\bar{B}^2 - i\frac{J_y}{\sqrt{N}}\bar{B}\right],$$

(17)

where $\bar{B} = \sqrt{N}\hat{b}$ and $D \equiv e^{-\frac{\delta}{N}}$ has been used. As in the thermodynamic limit, J_z/N just yields a constant; the first term in the last row can be seen as an all-to-all interaction between the environmental oscillators, which only depends in a bounded fashion on the LMG parameters h and γ_x. Since it is quadratic, it can be formally transformed away by a suitable global Bogoliubov transform $c_k = \sum_q(u_{kq}b_q + v_{kq}b_q^\dagger)$ of all reservoir oscillators, which results in

$$\bar{H}_{\text{tot}} \approx -hJ_z - \frac{\gamma_x}{N}J_x^2 + \sum_k \tilde{\nu}_k b_k^\dagger b_k + h\frac{iJ_y}{\sqrt{N}}\sum_k(h_k b_k - h_k^* b_k^\dagger),$$

(18)

and where $h_k \in \mathbb{C}$ are the transformed reservoir couplings and $\tilde{\nu}_k$ the transformed reservoir energies. In the case of weak coupling to the reservoir which is assumed here, however, we will simply neglect the $\bar{B}^2$ term since it is then much smaller than the linear $\bar{B}$ term.

2. System Hamiltonian diagonalization

To proceed, we first consider the normal phase $\gamma_x < h$. We first apply the Holstein-Primakoff transformation to the total Hamiltonian; compare Appendix A. Since in the normal phase the vanishing displacement implies $a = b$, this yields

$$\bar{H}_{\text{tot,N}}^{(\text{HP})} = -\frac{h}{2}N + \left(h - \frac{\gamma_x}{2}\right)a^\dagger a - \frac{\gamma_x}{4}(a^{\dagger 2} + a^2 + 1)$$
$$+ \sum_k \tilde{\nu}_k b_k^\dagger b_k + \frac{h}{2}(a - a^\dagger)\sum_k(h_k b_k - h_k^* b_k^\dagger). \quad (19)$$

Here, the main difference is that the system-reservoir interaction now couples to the momentum of the LMG oscillator mode and not the position. Applying yet another Bogoliubov transform $a = \cosh[\varphi(h, \gamma_x)]d + \sinh[\varphi(h, \gamma_x)]d^\dagger$ with the same parameters as in Table I eventually yields a Hamiltonian of a single diagonalized oscillator coupled via its momentum to a reservoir.

Analogously, the symmetry-broken phase $\gamma_x > h$ is treated with a finite displacement as outlined in Appendix A. The requirement that in the system Hamiltonian all terms proportional to $\sqrt{N}$ should vanish, yields the same known displacement (8). One arrives at a Hamiltonian of the form

$$\bar{H}_{\text{tot,S}}^{(\text{HP})} = -\frac{h^2 + \gamma_x^2}{4\gamma_x}N + \frac{5\gamma_x - 3h}{4}a^\dagger a + \frac{3\gamma_x - 5h}{8}(a^2 + a^{\dagger 2})$$
$$+ \frac{\gamma_x - 3h}{8} + \sum_k \tilde{\nu}_k b_k^\dagger b_k + \frac{h}{2}\sqrt{1 - |\alpha(h, \gamma_x)|^2}$$
$$\times (a - a^\dagger)\sum_k(h_k b_k - h_k^* b_k^\dagger). \quad (20)$$

Using a Bogoliubov transformation to new bosonic operators d, the system part in the above equation can be diagonalized again.

TABLE III. Additional parameters of the diagonalization procedure of H_{LMG} in the polaron frame for the normal phase ($\gamma_x < h$, second column) and symmetry-broken phase ($\gamma_x > h$, last column). Note that $\varphi(h, \gamma_x)$ (see Table I) is evaluated at the original spin-spin coupling γ_x.

	Normal: $\gamma_x < h$	Symmetry broken: $\gamma_x > h$
$\bar{C}_3(h, \gamma_x)$	h	$h\sqrt{\frac{1}{2}\left(1 + \frac{h}{\gamma_x}\right)}$
$\bar{A}(h, \gamma_x)$	$\frac{\bar{C}_3(h,\gamma_x)}{2}\exp[-\varphi(h,\gamma_x)]$	

Thus, in both phases, the Hamiltonian acquires the generic form

$$\bar{H}_{\text{tot}}^{(\text{HP})} = \omega(h, \gamma_x)d^\dagger d - NC_1(h, \gamma_x) + C_2(h, \gamma_x)$$
$$+ \bar{A}(h, \gamma_x)(d - d^\dagger)\sum_k\left(h_k b_k - h_k^* b_k^\dagger\right) + \sum_k \tilde{\nu}_k b_k^\dagger b_k,$$

(21)

where the system-reservoir coupling modification $\bar{A}(h, \gamma_x)$ is found in Table III.

To this form, we can directly apply the derivation of the standard quantum-optical master equation.

3. Master equation

In the polaron-transformed interaction Hamiltonian, we now observe the factor $\bar{A}(h, \gamma_x)$, which depends on h and γ_x; see Tables III and I. This factor is suppressed as one approaches the shifted critical point; it vanishes there identically. Near the shifted QPT, its square $\bar{A}^2(h, \gamma_x)$ shows the same scaling behavior as the system gap $\omega(h, \gamma_x)$, such that in the polaron frame, the system-reservoir interaction strength is adaptively scaled down with the system Hamiltonian, and a naive master-equation approach can be applied in this frame.

From either the normal phase or the symmetry-broken phase, we arrive at the following generic form of the system density matrix master equation:

$$\dot{\rho}(t) = -i[H_{\text{LMG}}^{\text{HP}}(h, \gamma_x), \rho] + \bar{F}_e \mathcal{D}(d)\rho + \bar{F}_a \mathcal{D}(d^\dagger)\rho,$$
$$\bar{F}_e = \bar{A}^2(h, \gamma_x)\bar{\Gamma}(\omega(h, \gamma_x))[1 + n_B(\omega(h, \gamma_x))],$$
$$\bar{F}_a = \bar{A}^2(h, \gamma_x)\bar{\Gamma}(\omega(h, \gamma_x))n_B(\omega(h, \gamma_x)). \quad (22)$$

Here, $\bar{\Gamma}(\omega) = 2\pi\sum_k|h_k|^2\delta(\omega - \tilde{\nu}_k)$ denotes the transformed spectral density, which is related to the original spectral density via the Bogoliubov transform that expresses the c_k operators in terms of the b_k operators, and $n_B(\omega)$ again denotes the Bose distribution. The mapping from the reservoir modes c_k to the new reservoir modes b_k has been represented in an implicit form, but in general it will be a general multimode Bogoliubov transformation [76,77] with a sophisticated solution.

However, if hg_k/ν_k is small in comparison to the reservoir frequencies ν_k, the Bogoliubov transform will hardly change the reservoir oscillators and thereby be close to the identity. Then, one will approximately recover $\bar{\Gamma}(\omega) \approx \Gamma(\omega)$. Even if this assumption is not fulfilled, we note from the general form of the master equation that the steady state will just be the thermalized system—with renormalized parameters depending on $\Gamma(\omega)$, h, and γ_x. Therefore, it will not depend

on the structure of $\bar{\Gamma}(\omega)$—although transient observables may depend on this transformed spectral density as well. In our results, we will therefore concentrate on a particular form of $\Gamma(\omega)$ only and neglect the implications for $\bar{\Gamma}(\omega)$.

IV. RESULTS

To apply the polaron-transform method, we require that all involved limits converge. All reasonable choices for a spectral density (12) will lead to convergence of the renormalized spin-spin interaction (4). However, convergence of the external field renormalization (15) may require subtle discussions on the order of the thermodynamic limits in the system ($N \rightarrow \infty$) and reservoir ($\sum_k g_k^2[\ldots] \rightarrow \frac{1}{2\pi} \int \Gamma(\omega)[\ldots]d\omega$), respectively. These discussions can be avoided if the spectral density grows faster than quadratically for small energies, e.g.,

$$\Gamma(\omega) = \eta \frac{\omega^3}{\omega_c^2} \exp(-\omega/\omega_c), \qquad (23)$$

where ω_c is a cutoff frequency and η is a dimensionless coupling strength. With this choice, the renormalized all-to-all interaction (4) becomes

$$\tilde{\gamma}_x = \gamma_x - \frac{\eta \omega_c}{\pi}, \qquad (24)$$

such that the QPT position given by Eq. (4) is shifted to $\gamma_x^{\mathrm{cr}} \rightarrow h + \frac{\eta \cdot \omega_c}{\pi}$.

We emphasize again that—independent of the spectral density—both derived master equations (11) and (22) let the system evolve towards the respective thermal state,

$$\rho = \frac{\exp\left[-\beta H_{\mathrm{LMG}}^{\mathrm{HP}}(h, \tilde{\gamma}_x)\right]}{Z}, \quad \bar{\rho} = \frac{\exp\left[-\beta H_{\mathrm{LMG}}^{\mathrm{HP}}(h, \gamma_x)\right]}{\bar{Z}}, \qquad (25)$$

in the original and polaron frame, respectively, where β is the inverse temperature of the bath and $Z/\bar{Z}$ are the respective normalization constants.

The difference between the treatments is therefore that within the BMS treatment (11), the rates may diverge and the system parameters are renormalized. The divergence of rates within the BMS treatment would also occur for a standard initial Hamiltonian. To illustrate this main result, we discuss a number of conclusions that can be derived from it below.

A. Magnetization

In general, the role of temperature in connection with the thermal phase transition in models such as LMG or Dicke has been widely studied using partition sums or by using naive BMS master equations [78–81]. Since in our case the stationary system state is just the thermalized one, standard methods (compare Appendix C) just analyzing the canonical Gibbs state of the isolated LMG model can be used to obtain stationary expectation values such as the magnetization. For the polaron approach, we obtain

$$\langle J^z \rangle = -\frac{\partial E_0(h, \gamma_x)}{\partial h} - \frac{1}{e^{\beta \omega(h, \gamma_x)} - 1} \frac{\partial \omega(h, \gamma_x)}{\partial h}, \qquad (26)$$

where $E_0(h, \gamma_x) = C_2(h, \gamma_x) - NC_1(h, \gamma_x)$ is the ground-state energy and $\omega(h, \gamma_x)$ the energy splitting; compare Table I. The
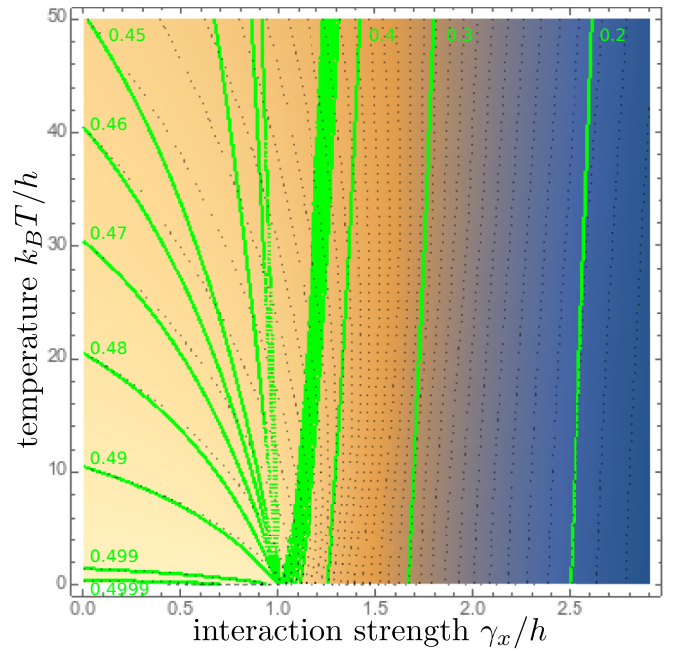

FIG. 2. Contour plot of the magnetization density $\langle J^z \rangle / N$ vs spin-spin interaction γ_x and temperature $k_B T$ for $N = 1000$. At the critical point $\gamma_x = h$, the magnetization density at low temperatures (bottom) suddenly starts to drop from a constant value in the normal phase (left) to a decaying curve in the symmetry-broken phase (right) as predicted by (27). At higher temperatures, the transition is smoother and the predictions from the bosonic representation [solid green contours, based on Eq. (26)] and the finite-size numerical calculation of the partition function [dashed contours, based on the Gibbs state with Eq. (2)] disagree for $\gamma_x \approx h$. For the finite-size calculation, weak coupling has been assumed, $k_B T \ll N \omega_c / \eta$, such that $U_p^\dagger J_z U_p \approx J_z$ instead of (B4).

quantum-critical nature is demonstrated by the first (ground-state) contribution, where the nonanalytic dependence of the ground-state energy on the external field strength will map to the magnetization. The second contribution is temperature dependent. In particular, in the thermodynamic limit $N \rightarrow \infty$, only a part of the ground-state contribution remains and we obtain

$$\lim_{N \rightarrow \infty} \frac{\langle J^z \rangle}{N} \rightarrow \frac{1}{2} \begin{cases} 1 & : \quad h > \gamma_x \\ \frac{h}{\gamma_x} & : \quad \gamma_x > h. \end{cases} \qquad (27)$$

For finite system sizes, however, finite-temperature corrections exist. In Fig. 2, we show a contour plot of the magnetization density $\langle J^z \rangle / N$ from the exact numerical calculation of the partition function (dashed contours) and compare with the results from the bosonic representation (solid green contours). We see, in the contour lines of the magnetization, convincing agreement between the curves of the bosonic representation (solid green) and the finite-size calculation (dashed black) only for very low temperatures or away from the critical point. The disagreement for $\gamma_x \approx h$ and $T > 0$ can be attributed to the fact that the bosonization for finite sizes only captures the lowest-energy eigenstates well, whereas in this region also the higher eigenstates become occupied. However, it is clearly visible that in the low-temperature regime, the magnetization
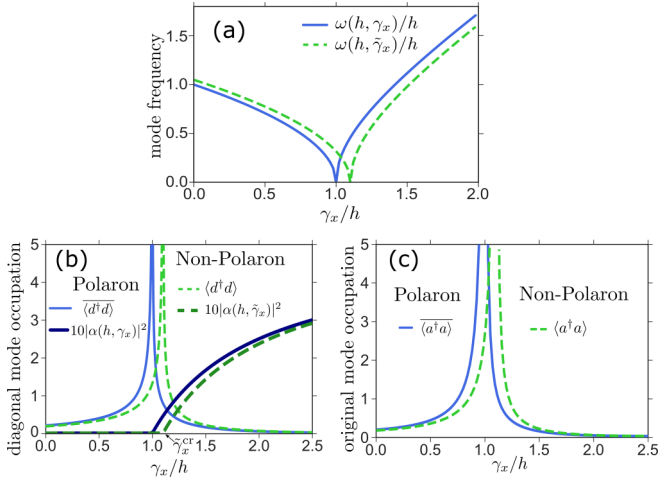
FIG. 3. (a) LMG oscillator frequency $\omega(h, \gamma_x)$ or $\omega(h, \tilde{\gamma}_x)$; (b) diagonal frame steady-state mode occupations $\overline{\langle d^\dagger d \rangle}$ ($\langle d^\dagger d \rangle$); and (c) nondiagonal frame steady-state mode occupations $\langle a^\dagger a \rangle$($\langle a^\dagger a \rangle$) for the polaron (solid) and nonpolaron (dashed) master equations. Divergent mode occupations indicate the position of the QPT where the excitation frequency vanishes. For the polaron treatment, the QPT position stays at $\gamma_x/h = 1$ just as in the isolated LMG model, in contrast to the shift predicted by the BMS master equation. Parameters: $\eta = 2\pi(0.1)$, $\omega_c = 0.5h$, $\beta = 1.79/h$.

density will drop suddenly when $\gamma_x \geqslant h$, such that the QPT can be detected at correspondingly low temperatures. At high temperatures, the magnetization density falls off smoothly with increasing spin-spin interaction.

B. Mode occupation

The master equations appear simple only in a displaced and rotated frame. When transformed back, the steady-state populations $\langle d^\dagger d \rangle = \text{Tr}\{d^\dagger d \rho\}$ and $\overline{\langle d^\dagger d \rangle} = \text{Tr}\{d^\dagger d \bar{\rho}\}$ actually measure displacements around the mean field. Figure 3 compares the occupation number and system frequency with (solid) and without (dashed) polaron transform. Figure 3(a) demonstrates that the LMG energy gap is in the BMS treatment strongly modified by dissipation, such that in the vicinity of the closed QPT, the nonpolaron and polaron treatments lead to very different results. Figure 3(b) shows the fluctuations in the diagonal basis $\overline{\langle d^\dagger d \rangle}$ ($\langle d^\dagger d \rangle$) around the mean field $\alpha(h, \gamma_x)$ [or $\alpha(h, \tilde{\gamma}_x)$] in the polaron (or nonpolaron) frame. Finally, Fig. 3(c) shows the mode occupation $\langle a^\dagger a \rangle = \sinh^2[\varphi(h, \gamma_x)] + 2\cosh^2[\varphi(h, \gamma_x)]\langle d^\dagger d \rangle$ (and analogous in the symmetry-broken phase) in the nondiagonal basis. These are directly related to the deviations of the J_z expectation value from its mean-field solution; compare Appendix A. Since the frequency $\omega(h, \tilde{\gamma}_x)$ (Table I) vanishes at $\gamma_x = h + \frac{\eta \cdot \omega_c}{\pi}$ in the nonpolaron frame, the BMS approximations break down around the original QPT position; see dashed line in Fig. 3(a). Mode occupations in both the diagonal and nondiagonal bases diverge at the QPT point; see the dashed lines in Figs. 3(b) and 3(c). In particular, in the polaron frame, the fluctuation divergence occurs around the original quantum critical point at $\gamma_x = h$; see the solid lines in Fig. 3.
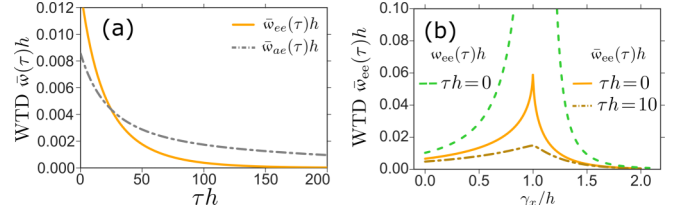

FIG. 4. Waiting-time distributions (WTDs) between two emission (absorption and emission) events (a) $\bar{w}_{ee(ae)}$ (solid, dot-dashed line) calculated in the polaron frame as a function of τ for a fixed γ_x value and (b) distribution $\bar{w}_{ee}$ as a function of γ_x for two different fixed τ values. Additionally, the WTD in the nonpolaron frame is shown in (b) for $\tau = 0$ case (dashed line), which wrongly diverges around the shifted critical point. At the true critical point, a nonanalytic dependence of the distribution on the intraspin-coupling strength γ_x is clearly visible; within the polaron treatment, however, all WTDs remain finite. Parameters: $\eta = 2\pi(0.1)$, $\omega_c = 0.5h$, $\beta = 1.79/h$, (a) $\gamma_x = 0.5h$.

C. Waiting times

The coupling to the reservoir does not only modify the system properties, but may also lead to the emission or absorption of reservoir excitations (i.e., photons or phonons depending on the model implementation), which can, in principle, be measured independently. Classifying these events into classes ν describing, e.g., emissions or absorptions, the waiting-time distribution between two such system-bath exchange processes of type μ after ν is characterized by [82]

$$w_{\mu\nu}(\tau) = \frac{\text{Tr}[\mathcal{J}_\mu \exp(\mathcal{L}_0 \tau)\mathcal{J}_\nu \rho]}{\text{Tr}(\mathcal{J}_\nu \rho)}. \tag{28}$$

Here, $\mathcal{J}_\mu$, $\mathcal{L}_0$ are superoperators describing the jump μ and the no-jump evolution $\mathcal{L}_0$. For example, in master equation (11), there are only two distinct types of jumps, i.e., emission "e" and absorption "a". Their corresponding superoperators are then acting as

$$\mathcal{J}_e\rho = F_e d\rho d^\dagger, \quad \mathcal{J}_a\rho = F_a d^\dagger \rho d,$$

$$\mathcal{L}_0\rho = -i[\omega d^\dagger d, \rho] - \frac{F_e}{2}\{d^\dagger d, \rho\} - \frac{F_a}{2}\{dd^\dagger, \rho\}, \tag{29}$$

such that the total Liouvillian is decomposable as $\mathcal{L} = \mathcal{L}_0 + \mathcal{J}_e + \mathcal{J}_a$. The same equations are valid in the polaron frame (22), just with the corresponding overbar on the variables.

It is straightforward to go to a frame where the Hamiltonian dynamics is absorbed, $\tilde{\rho} = e^{+i\omega t d^\dagger d}\rho e^{-i\omega t d^\dagger d}$; we see that the whole Liouvillian in this frame $\tilde{\mathcal{L}}$ is just proportional to the spectral density, evaluated at the system transition frequency ω. Thereby, it enters as a single parameter; a different spectral density could be interpreted as a rescaling $\Gamma(\omega) \to \alpha\Gamma(\omega)$, which would imply $\mathcal{L}_0 \to \alpha\mathcal{L}_0$ and $\mathcal{J}_\mu \to \alpha\mathcal{J}_\mu$. These transformations would only lead to a trivial stretching of the waiting-time distribution $w_{\mu\nu}(\tau) \to \alpha w_{\mu\nu}(\alpha\tau)$; compare, also, Eq. (D5).

Since the LMG Hamiltonian and the steady state (25) are diagonal, analytic expressions for the waiting-time distributions can be derived; see Appendix D. In Fig. 4, we show two waiting-time distributions $\bar{w}_{ee(ae)}$ as a function of time τ for fixed coupling strength γ_x [Fig. 4(a)] and the

repeated-emission waiting-time distribution $\bar{w}_{ee}(\tau)$ as a function of γ_x for two fixed waiting times τ [Fig. 4(b)]. A typical feature of a thermal state is bunching of emitted photons, which we see in Fig. 4(a): After an emission event, the same event has the highest probability for $\tau \to 0$, thus immediately. When looking at waiting-time distributions of different phases, such as Fig. 4(a), a significant difference is not visible. However, by fixing the waiting time τ and varying γ_x, we find that the waiting times have their maximum at the position of QPT; see Fig. 4(b). Essentially, this is related to the divergence of $n_B(\omega)$ when the energy gap vanishes. Whereas the nonpolaron treatment predicts a divergence of waiting times around the critical point $\tilde{\gamma}_x^{cr}$ [see the dashed curve in Fig. 4(b)], the waiting times within the polaron approach remain finite but depend nonanalytically on the Hamiltonian parameters.

Therefore, the quantum-critical behavior is not only reflected in system-intrinsic observables such as mode occupations but also in reservoir observables such as the statistics of photoemission events.

V. SUMMARY

We have investigated the open LMG model by using a polaron-transform technique that also allows us to address the vicinity of the critical point.

First, within the polaron treatment, we have found that the position of the QPT is robust when starting from an initial Hamiltonian with a lower spectral bound. This shows that the choice of the starting Hamiltonian should be discussed with care for critical models, even when treated as weakly coupled.

Second, whereas far from the QPT the approach presented here reproduces naive master-equation treatments, it also remains valid in the vicinity of the QPT. In the transformed frame, the effective interaction scales with the energy gap of the system Hamiltonian, which admits a perturbative treatment at the critical point. We therefore expect that the polaron–master-equation approach is also applicable to other models that bilinearly couple to bosonic reservoirs via position operators.

Interestingly, we obtained that for a single reservoir, the stationary properties are determined by those of the isolated system alone, such that a standard analysis applies.

The critical behavior (and its possible renormalization) can be detected with system observables such as magnetization or mode occupations, but is also visible in reservoir observables such as waiting-time distributions, which remain finite in the polaron frame. We hope that our study of the LMG model paves the way for further quantitative investigations of dissipative quantum-critical systems, e.g., by capturing higher eigenstates by augmented variational polaron treatments [83] or by investigating the nonequilibrium dynamics of critical setups.

APPENDIX A: THERMODYNAMIC LIMIT OF LARGE SPIN OPERATORS

Without any displacement, the Holstein-Primakoff representation leads to a simple large-N expansion,

$$J_- \approx \sqrt{N}b^\dagger, \quad J_+ \approx \sqrt{N}b, \quad J_z = \frac{N}{2} - b^\dagger b, \quad (A1)$$

where we have neglected terms that vanish in the thermodynamic limit. Insertion of these approximations lead to the Hamiltonians for the normal phase and, in effect, no term of the order of $\sqrt{N}$ occurs in the Hamiltonian.

In the symmetry-broken phase, one allows for a displacement $b = a + \alpha\sqrt{N}$ with bosonic operators a and, in general, complex number α. Then, the large-N expansion of the large spin operators is more complicated,

$$
\begin{aligned}
J_- &\approx N\alpha^*\sqrt{1-|\alpha|^2} + \sqrt{N}\sqrt{1-|\alpha|^2} \\
&\times \left[a^\dagger - \frac{1}{2}\frac{(\alpha^*)^2 a + |\alpha|^2 a^\dagger}{1-|\alpha|^2} \right] - \frac{\sqrt{1-|\alpha|^2}}{2(1-|\alpha|^2)} \\
&\times \left[\alpha(a^\dagger)^2 + 2\alpha^* a^\dagger a + \frac{\alpha^*(\alpha^* a + \alpha a^\dagger)^2}{4(1-|\alpha|^2)} \right], \\
J_+ &\approx N\alpha\sqrt{1-|\alpha|^2} + \sqrt{N}\sqrt{1-|\alpha|^2}\left[a - \frac{1}{2}\frac{\alpha^2 a^\dagger + |\alpha|^2 a}{1-|\alpha|^2} \right] \\
&- \frac{\sqrt{1-|\alpha|^2}}{2(1-|\alpha|^2)}\left[\alpha^* a^2 + 2\alpha a^\dagger a + \frac{\alpha(\alpha^* a + \alpha a^\dagger)^2}{4(1-|\alpha|^2)} \right], \\
J_z &= N\left(\frac{1}{2} - |\alpha|^2 \right) - \sqrt{N}(\alpha^* a + \alpha a^\dagger) - a^\dagger a. \quad (A2)
\end{aligned}
$$

For consistency, one can check that by setting $\alpha \to 0$, the previous representation is reproduced. Insertion of this expansion leads to the Hamiltonians for the symmetry-broken phase, and the displacement α is chosen such that the $\sqrt{N}$ terms in the LMG Hamiltonian vanish. One might be tempted to neglect the last expansion terms in $J_\pm$ from the beginning, as these operators enter the Hamiltonian always with a factor of $1/\sqrt{N}$. However, we stress that in terms such as J_x^2/N, they will yield a nonvanishing contribution and thus need to be considered to obtain the correct spectra of the LMG model.

APPENDIX B: POLARON TRANSFORM

Here we provide more details of how to derive Eq. (14) in the main text. Using the Hadamard lemma,

$$
\begin{aligned}
e^{+X}Ye^{-X} &= \sum_{m=0}^\infty \frac{1}{m!}[X,Y]_m, \\
[X,Y]_m &= [X,[X,Y]_{m-1}], \quad [X,Y]_0 = Y, \quad (B1)
\end{aligned}
$$

one can see that the polaron transform (13) leads to

$$U_p^\dagger c_k U_p = c_k - \frac{J_x}{\sqrt{N}}\frac{g_k}{\nu_k}, \quad (B2)$$

and analogously for the transformation of the creation operator. Furthermore, it is trivial to see that $U_p^\dagger J_x U_p = J_x$. From this, it directly follows that the polaron transform of the

interaction and reservoir Hamiltonian becomes

$$
U_p^\dagger \left(c_k^\dagger + \frac{g_k}{\sqrt{N}\nu_k} J_x \right) \left(c_k + \frac{g_k}{\sqrt{N}\nu_k} J_x \right) U_p = c_k^\dagger c_k. \quad \text{(B3)}
$$

In addition, the polaron transform of J_z has to be calculated, which yields, via the commutation relations $[J_x, J_y] = iJ_z$, the relation

$$
U_p^\dagger J_z U_p = J_z \cosh(\hat{B}) - iJ_y \sinh(\hat{B}), \quad \text{(B4)}
$$

where $\hat{B}$ is defined in (13) in the main text.

Therefore, the full polaron-transformed Hamiltonian H_{tot} becomes

$$
U_p^\dagger H_{\text{tot}} U_p = -hD J_z - \frac{\gamma_x}{N} J_x^2 + \sum_k \nu_k b_k^\dagger b_k
$$
$$
- h\{J_z[\cosh(\hat{B}) - D] - iJ_y \sinh(\hat{B})\},
$$

such that there is no rescaling of the spin-spin interaction γ_x. We have also already inserted the temperature-dependent shift D, which is necessary in order to ensure that the first-order expectation values of the system-reservoir coupling operators vanish, eventually yielding Eq. (14) in the main text. For the sinh term, this is not necessary as its expectation value vanishes anyhow.

APPENDIX C: MAGNETIZATION

It is well known that for a Hamiltonian depending on an external parameter λ (which for our model could be h or γ_x), the canonical partition function

$$
Z = \text{Tr}\{e^{-\beta H(\lambda)}\} \quad \text{(C1)}
$$

allows one to evaluate the thermal expectation value of particular operators,

$$
\frac{-1}{\beta} \frac{\partial \ln Z}{\partial \lambda} = \frac{-1}{Z\beta} \text{Tr}\left\{ \frac{\partial}{\partial \lambda} e^{-\beta H(\lambda)} \right\}
$$
$$
= \frac{1}{Z} \sum_{n=1}^\infty \frac{(-\beta)^{n-1}}{(n-1)!} \text{Tr}\left\{ \frac{\partial H(\lambda)}{\partial \lambda} H^{n-1}(\lambda) \right\}
$$
$$
= \frac{1}{Z} \text{Tr}\left\{ \frac{\partial H(\lambda)}{\partial \lambda} e^{-\beta H(\lambda)} \right\} = \left\langle \frac{\partial H(\lambda)}{\partial \lambda} \right\rangle, \quad \text{(C2)}
$$

where we have used the invariance of the trace under cyclic permutations to sort all derivatives of $H(\lambda)$ to the left.

In particular, for a harmonic oscillator $H = E_0(\lambda) + \omega(\lambda)a^\dagger(\lambda)a(\lambda)$ with bosonic operators $a(\lambda)$, the partition function becomes

$$
Z = \frac{e^{-\beta E_0(\lambda)}}{1 - e^{-\beta \omega(\lambda)}}. \quad \text{(C3)}
$$

With $\lambda \to -h$, this eventually leads to Eq. (26) in the main text.

APPENDIX D: WAITING-TIME DISTRIBUTION

Starting from the spectral decomposition of a thermal state in terms of Fock states,

$$
\rho = \frac{e^{-\beta \omega d^\dagger d}}{\text{Tr}\{e^{-\beta \omega d^\dagger d}\}} = \sum_{n=0}^\infty P_n |n\rangle \langle n|,
$$
$$
P_n = \left(\frac{n_B}{1 + n_B} \right)^n \frac{1}{1 + n_B}, \quad \text{(D1)}
$$

with the shorthand notation $n_B = [e^{\beta \omega} - 1]^{-1}$, it is straightforward to compute the action of the emission or absorption jump superoperators,

$$
\mathcal{J}_e \rho = F_e \sum_{n=0}^\infty P_{n+1}(n+1) |n\rangle \langle n|,
$$
$$
\mathcal{J}_a \rho = F_a \sum_{n=1}^\infty P_{n-1} n |n\rangle \langle n|, \quad \text{(D2)}
$$

which also implies

$$
\text{Tr}\{\mathcal{J}_e \rho\} = \text{Tr}\{\mathcal{J}_a \rho\} = \Gamma n_B (1 + n_B), \quad \text{(D3)}
$$

where $\Gamma = A^2(h, \tilde{\gamma}_x) \Gamma(\omega(h, \tilde{\gamma}_x))$ or $\Gamma = \bar{A}^2(h, \gamma_x) \bar{\Gamma}(\omega(h, \gamma_x))$ in the main text. Since $\mathcal{L}_0$ does not induce transitions between different Fock states, its action on a diagonal density matrix can be computed via

$$
e^{\mathcal{L}_0 t} |n\rangle \langle n| = e^{-[(1+n_B)n + n_B(1+n)]\Gamma t} |n\rangle \langle n|, \quad \text{(D4)}
$$

which implies, for the relevant terms,

$$
w_{ee}(\tau) = \frac{2\Gamma n_B(1 + n_B)e^{(2+3n_B)\Gamma\tau}}{[(1 + n_B)e^{(1+2n_B)\Gamma\tau} - n_B]^3},
$$
$$
w_{ae}(\tau) = \frac{\Gamma n_B e^{(2+3n_B)\Gamma\tau}[n_B + (1 + n_B)e^{(1+2n_B)\Gamma\tau}]}{[(1 + n_B)e^{(1+2n_B)\Gamma\tau} - n_B]^3},
$$
$$
w_{ea}(\tau) = \frac{\Gamma(1 + n_B)e^{(1+n_B)\Gamma\tau}[n_B + (1 + n_B)e^{(1+2n_B)\Gamma\tau}]}{[(1 + n_B)e^{(1+2n_B)\Gamma\tau} - n_B]^3},
$$
$$
w_{aa}(\tau) = \frac{2\Gamma n_B(1 + n_B)e^{(2+3n_B)\Gamma\tau}}{[(1 + n_B)e^{(1+2n_B)\Gamma\tau} - n_B]^3}. \quad \text{(D5)}
$$

For consistency, we note that the normalization conditions $\int [w_{ae}(\tau) + w_{ee}(\tau)]d\tau = 1$ and $\int [w_{aa}(\tau) + w_{ea}(\tau)]d\tau = 1$ always hold, which simply reflects the fact that only emission or absorption processes can occur. Furthermore, in the low-temperature limit $n_B \to 0$, only the conditional waiting-time distribution for emission after absorption can survive, $w_{ea} \to \Gamma e^{-\Gamma\tau}$: Once a photon has been absorbed from the reservoir, it must be emitted again since no further absorption is likely to occur. For $\tau \gg 1$, all waiting-time distributions $\bar{w}_{\mu\nu}$ decay to zero.

[1] S. Sachdev, *Quantum Phase Transitions* (Wiley Online Library, New York, 2007).

[2] P. Ribeiro, J. Vidal, and R. Mosseri, Phys. Rev. Lett. **99**, 050402 (2007).

[3] M. A. Bastarrachea-Magnani, S. Lerma-Hernández, and J. G. Hirsch, Phys. Rev. A **89**, 032102 (2014).

[4] N. Lambert, C. Emary, and T. Brandes, Phys. Rev. Lett. **92**, 073602 (2004).

[5] K. Baumann, C. Guerlin, F. Brennecke, and T. Esslinger, Nature (London) **464**, 1301 (2010).

[6] K. Baumann, R. Mottl, F. Brennecke, and T. Esslinger, Phys. Rev. Lett. **107**, 140402 (2011).

[7] F. Brennecke, R. Mottl, K. Baumann, R. Landig, T. Donner, and T. Esslinger, Proc. Natl. Acad. Sci. **110**, 11763 (2013).

[8] T. Zibold, E. Nicklas, C. Gross, and M. K. Oberthaler, Phys. Rev. Lett. **105**, 204101 (2010).

[9] H. Ritsch, P. Domokos, F. Brennecke, and T. Esslinger, Rev. Mod. Phys. **85**, 553 (2013).

[10] R. H. Dicke, Phys. Rev. **93**, 99 (1954).

[11] L. Fusco, M. Paternostro, and G. De Chiara, Phys. Rev. E **94**, 052122 (2016).

[12] S. Çakmak, F. Altintas, and Ö. E. Müstecaplıoğlu, Eur. Phys. J. Plus **131**, 197 (2016).

[13] Y.-H. Ma, S.-H. Su, and C.-P. Sun, Phys. Rev. E **96**, 022143 (2017).

[14] M. Kloc, P. Cejnar, and G. Schaller, Phys. Rev. E **100**, 042126 (2019).

[15] V. M. Bastidas, C. Emary, B. Regler, and T. Brandes, Phys. Rev. Lett. **108**, 043003 (2012).

[16] G. Engelhardt, V. M. Bastidas, C. Emary, and T. Brandes, Phys. Rev. E **87**, 052110 (2013).

[17] V. M. Bastidas, G. Engelhardt, P. Pérez-Fernández, M. Vogl, and T. Brandes, Phys. Rev. A **90**, 063628 (2014).

[18] O. Acevedo, L. Quiroga, F. Rodríguez, and N. Johnson, New J. Phys. **17**, 093005 (2015).

[19] W. Kopylov, G. Schaller, and T. Brandes, Phys. Rev. E **96**, 012153 (2017).

[20] S. Campbell, Phys. Rev. B **94**, 184403 (2016).

[21] M. O. Scully, *Quantum Optics* (Cambridge University Press, Cambridge, 1997).

[22] T. E. Lee, C.-K. Chan, and S. F. Yelin, Phys. Rev. A **90**, 052109 (2014).

[23] W. Kopylov, C. Emary, and T. Brandes, Phys. Rev. A **87**, 043840 (2013).

[24] S. Mostame, G. Schaller, and R. Schützhold, Phys. Rev. A **76**, 030304(R) (2007).

[25] S. Mostame, G. Schaller, and R. Schützhold, Phys. Rev. A **81**, 032305 (2010).

[26] J. Klinder, H. Keßler, M. Wolke, L. Mathey, and A. Hemmerich, Proc. Natl. Acad. Sci. **112**, 3290 (2015).

[27] J. Lebreuilly, A. Chiocchetta, and I. Carusotto, Phys. Rev. A **97**, 033603 (2018).

[28] F. M. Faulstich, M. Kraft, and A. Carmele, J. Mod. Opt. **65**, 1323 (2017).

[29] W. Kopylov and T. Brandes, New J. Phys. **17**, 103031 (2015).

[30] J. Kabuss, F. Katsch, A. Knorr, and A. Carmele, J. Opt. Soc. Am. B **33**, C10 (2016).

[31] H.-P. Breuer and F. Petruccione, *The Theory of Open Quantum Systems* (Oxford University Press, Oxford, 2002).

[32] M. Vogl, G. Schaller, and T. Brandes, Phys. Rev. Lett. **109**, 240402 (2012).

[33] G. Schaller, M. Vogl, and T. Brandes, J. Phys.: Condens. Matter **26**, 265001 (2014).

[34] G. Schaller, *Open Quantum Systems Far from Equilibrium* (Springer, Cham, 2014).

[35] A. Nazir and G. Schaller, in *Thermodynamics in the Quantum Regime – Recent Progress and Outlook*, Fundamental Theories of Physics, edited by F. Binder, L. A. Correa, C. Gogolin, J. Anders, and G. Adesso (Springer, Cham, 2019).

[36] P. Strasberg, G. Schaller, N. Lambert, and T. Brandes, New J. Phys. **18**, 073007 (2016).

[37] N. Meshkov, A. J. Glick, and H. J. Lipkin, Nucl. Phys. **62**, 199 (1965).

[38] G. D. Mahan, *Many-particle Physics* (Springer Science & Business Media, New York, 2013).

[39] L. Glazman and R. Shekhter, Sov. Phys. JETP **67**, 163 (1988).

[40] N. S. Wingreen, K. W. Jacobsen, and J. W. Wilkins, Phys. Rev. Lett. **61**, 1396 (1988).

[41] T. Brandes, Phys. Rep. **408**, 315 (2005).

[42] G. Schaller, T. Krause, T. Brandes, and M. Esposito, New J. Phys. **15**, 033032 (2013).

[43] M. Thorwart, E. Paladino, and M. Grifoni, Chem. Phys. **296**, 333 (2004).

[44] F. Wilhelm, S. Kleff, and J. Von Delft, Chem. Phys. **296**, 345 (2004).

[45] T. Brandes and T. Vorrath, Int. J. Mod. Phys. B **17**, 5465 (2003).

[46] M. A. Alcalde, M. Bucher, C. Emary, and T. Brandes, Phys. Rev. E **86**, 012101 (2012).

[47] T. Krause, T. Brandes, M. Esposito, and G. Schaller, J. Chem. Phys. **142**, 134106 (2015).

[48] P. Kirton and J. Keeling, Phys. Rev. Lett. **111**, 100404 (2013).

[49] M. Radonjić, W. Kopylov, A. Balaž, and A. Pelster, New J. Phys. **20**, 055014 (2018).

[50] M. J. Bhaseen, J. Mayoh, B. D. Simons, and J. Keeling, Phys. Rev. A **85**, 013817 (2012).

[51] D. Nagy, G. Szirmai, and P. Domokos, Phys. Rev. A **84**, 043637 (2011).

[52] M.-J. Hwang, P. Rabl, and M. B. Plenio, Phys. Rev. A **97**, 013825 (2018).

[53] J. Gelhausen and M. Buchhold, Phys. Rev. A **97**, 023807 (2018).

[54] H. Li, A. Piryatinski, J. Jerke, A. R. S. Kandada, C. Silva, and E. R. Bittner, Quantum Sci. Technol. **3**, 015003 (2017).

[55] S. Morrison and A. S. Parkins, Phys. Rev. Lett. **100**, 040403 (2008).

[56] R. Orús, S. Dusuel, and J. Vidal, Phys. Rev. Lett. **101**, 025701 (2008).

[57] M. Kochmański, T. Paszkiewicz, and S. Wolski, Eur. J. Phys. **34**, 1555 (2013).

[58] H. J. Lipkin, N. Meshkov, and A. Glick, Nucl. Phys. **62**, 188 (1965).

[59] A. Glick, H. Lipkin, and N. Meshkov, Nucl. Phys. **62**, 211 (1965).

[60] R. Gilmore and D. Feng, Nucl. Phys. A **301**, 189 (1978).

[61] F. Leyvraz and W. D. Heiss, Phys. Rev. Lett. **95**, 050402 (2005).

[62] A. V. Sorokin, V. M. Bastidas, and T. Brandes, Phys. Rev. E **90**, 042141 (2014).

[63] J. Vidal, G. Palacios, and C. Aslangul, Phys. Rev. A **70**, 062304 (2004).

[64] Y. Huang, T. Li, and Z.-qi Yin, Phys. Rev. A **97**, 012115 (2018).

[65] P. Ribeiro, J. Vidal, and R. Mosseri, Phys. Rev. E **78**, 021106 (2008).

[66] S. Dusuel and J. Vidal, Phys. Rev. B **71**, 224420 (2005).

[67] S. Dusuel and J. Vidal, Phys. Rev. Lett. **93**, 237204 (2004).

[68] S. Zimmermann, W. Kopylov, and G. Schaller, J. Phys. A: Math. Theor. **51**, 385301 (2018).

[69] T. Holstein and H. Primakoff, Phys. Rev. **58**, 1098 (1940).

[70] C. Emary and T. Brandes, Phys. Rev. E **67**, 066203 (2003).

[71] J. C. Louw, J. N. Kriel, and M. Kastner, Phys. Rev. A **100**, 022115 (2019).

[72] F. Dimer, B. Estienne, A. S. Parkins, and H. J. Carmichael, Phys. Rev. A **75**, 013804 (2007).

[73] C. Wang, J. Ren, and J. Cao, Sci. Rep. **5**, 11787 (2015).

[74] C. Wang and K.-W. Sun, Ann. Phys. **362**, 703 (2015).

[75] A. Garg, J. N. Onuchic, and V. Ambegaokar, J. Chem. Phys. **83**, 4491 (1985).

[76] C. Tsallis, J. Math. Phys. **19**, 277 (1978).

[77] Y. Tikochinsky, J. Math. Phys. **20**, 406 (1979).

[78] S. T. Tzeng, P. J. Ellis, T. Kuo, and E. Osnes, Nucl. Phys. A **580**, 277 (1994).

[79] M. Hayn and T. Brandes, Phys. Rev. E **95**, 012153 (2017).

[80] J. Wilms, J. Vidal, F. Verstraete, and S. Dusuel, J. Stat. Mech: Theory Expt. (2012) P01023.

[81] E. G. Dalla Torre, Y. Shchadilova, E. Y. Wilner, M. D. Lukin, and E. Demler, Phys. Rev. A **94**, 061802(R) (2016).

[82] T. Brandes, Ann. Phys. **17**, 477 (2008).

[83] D. P. S. McCutcheon, N. S. Dattani, E. M. Gauger, B. W. Lovett, and A. Nazir, Phys. Rev. B **84**, 081305(R) (2011).